

Figure 2 Variation of carbonyl index versus time of irradiation in a Xenotest-150 weatherometer (50% r.h. 45°C) for different batches of commercial unstabilized polypropylene film. Before irradiation the samples had relative fluorescence intensities at 340 nm:  $\blacktriangle$ , -1.0;  $\blacksquare$ ,  $\bullet$  -0.73;  $\square$ ,  $\triangle$  -0.44,  $\circ$ , -0.25 ( $E\lambda_{\max} = 230$  and 285 nm). All polymer samples were vacuum pressed at 190°C and had M.F.I. and Ti values of 20 and 25 ppm respectively

a correlation between initial  $\alpha,\beta$ -unsaturated carbonyl group concentration and rate of polymer photooxidation is due to the fact that their infra-red method was based on monitoring the broad band centred at 1685  $\text{cm}^{-1}$ . This absorption band can include a variety of unsaturated carbonylic groups such as carboxylic acids<sup>7</sup> that do not absorb light above 290 nm (see Figure 1)<sup>8</sup>. Consequently, these groups would not be expected to participate in the sun-light-induced oxidation of the polymer.

#### Experimental

The polypropylene films were irradiated in a Xenotest-150 weatherometer (Original Hanau, Quartzlamp-en, GmbH) set up for natural sun-light-

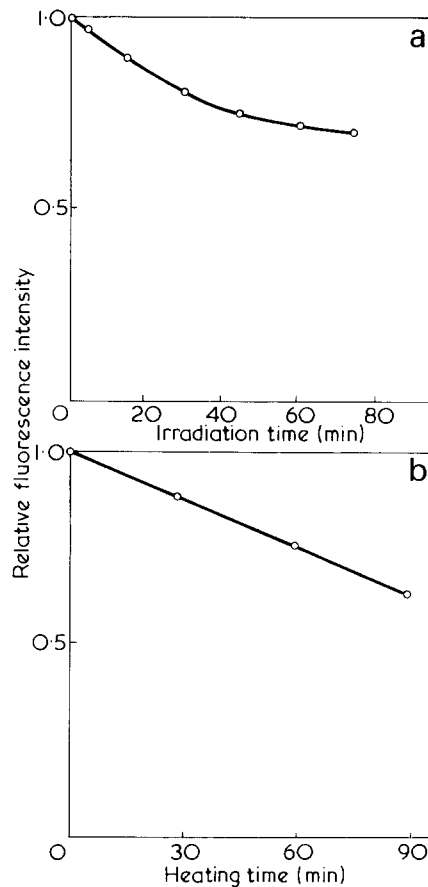


Figure 3 (a) Effect of irradiation in a Xenotest-150 weatherometer on the intensity of the fluorescence emission ( $\lambda_{\max} = 340$  nm) from commercial unstabilized polypropylene film (200  $\mu\text{m}$  thickness). (b) Effect of thermal treatment at 120°C under nitrogen on the intensity of the fluorescence emission from commercial unstabilized polypropylene film.  $E\lambda = 285$  nm

simulated exposure conditions (45°C; 50% relative humidity). A 1500 W xenon lamp is employed as the light source. The rate of photooxidation of the polymer films was measured by monitoring the build-up in the non-volatile carbonylic oxidation products absorbing at 1710  $\text{cm}^{-1}$  using a Perkin-Elmer 157G infra-red spectrophotometer. Carbonyl index =  $[(\log_{10} I_0/I_t)/d] \times 100$ ; where  $I_0$  = initial light intensity;  $I_t$  = transmitted light intensity;  $d$  = film thickness ( $\mu\text{m}$ ).

N. S. Allen and J. F. McKellar

Department of Chemistry and Applied Chemistry, University of Salford, Salford M5 4WT, Lancashire, UK  
(Received 9 May 1977)

#### References

- Allen, N. S., Cundall, R. B., Jones, M. W. and McKellar, J. F. *Chem. Ind.* 1976, p 110
- Allen, N. S., Homer, J. and McKellar, J. F. *Chem. Ind.* 1976, p 692
- Allen, N. S., Homer, J. and McKellar, J. F. *J. Appl. Polym. Sci.* in press
- Allen, N. S., McKellar, J. F. and Phillips, G. O. *Polym. Prepr.* 1977, p 375
- Allen, N. S. and McKellar, J. F. *Chem. Soc. Rev.* 1975, 4, 533
- Chakraborty, K. B. and Scott, G. *Polymer* 1977, 18, 98
- Bellamy, L. J. 'The Infra-red Spectra of Complex Molecules', Methuen, London, 1954, Ch 9 and 10
- 'Directory of Molecular Spectra - U.V. Atlas of Organic Compounds', Vols II and III, Butterworths, London, 1966

### Electric birefringence of sodium poly(L-glutamate) in water/organic solvent mixtures

Poly(L-glutamic acid)  $(\text{Glu})_n$ , is a synthetic polypeptide with ionizable side chains. The acid form adopts uncharged helical conformations in some organic solvents such as dimethylformamide and exhibits large electric birefringence<sup>1,2</sup>. In this case, the permanent dipole moment along the helix axis dominates in the mechanism of orientation in an electric field. When  $(\text{Glu})_n$  is ionized by adding alkali in aqueous solution, the situation is entirely different. At neutral or alkaline pH,  $(\text{Glu})_n$  assumes the 'charged coil' form. By lowering pH, a transition from coil to helix is induced<sup>3</sup>. Recently, Kobayasi and Ikegami<sup>4</sup> studied the changes of the specific Kerr constant and the birefrin-

gence relaxation time accompanied by the pH-induced helix-coil transition. The coil-to-helix transition is also induced by adding organic solvents such as dioxane<sup>5</sup> and methanol<sup>6</sup> to aqueous solutions of sodium poly(L-glutamate). In the present work we have studied the electric birefringence of sodium poly(L-glutamate) in water/organic solvent mixtures as a function of the solvent composition and the field strength.

Two samples of  $(\text{Glu})_n$  were used. Their degrees of polymerization ( $DP$ ) were estimated from the limiting viscosity number ( $[\eta]$ ) measured at 25°C, pH 7.3 in a 0.2 M NaCl solution, using the calibration of Wada<sup>7</sup>:

Sample	$[\eta]$ ( $\text{cm}^3/\text{g}$ )	$DP$
I	135	380
II	182	670

$(\text{Glu})_n$  was dissolved in sodium hydroxide solution and dialysed against distilled water. The mixtures were made up by adding organic solvent (methanol or ethylene glycol) to this original solution. The solvent composition was expressed as the volume percentage of organic solvent.

The apparatus and procedures for electric birefringence measurements have been described previously<sup>8,9</sup>. The

electric field was applied to the solution in a Kerr cell in the form of single rectangular pulses of up to 6 kV amplitude. The circular dichroism spectra were recorded with a JASCO J-20 recording spectropolarimeter at room temperature under constant nitrogen flush. The c.d. data were expressed in terms of molar ellipticity, based on the molecular weight of the amino-acid residue.

The steady-state electric birefringence ( $\Delta n$ ) of sodium poly(L-glutamate) solutions was determined as a function of the field strength ( $E$ ) at various solvent compositions. An example of  $\Delta n/\lambda c$  versus  $E^2$  plot is presented in Figure 1. Here  $\lambda$  is the wavelength of light ( $\lambda = 546$  nm in this experiment) and  $c$  is the concentration of sodium poly(L-glutamate) expressed as g/cm<sup>3</sup>. The initial slope of such a plot gives the specific Kerr constant defined by  $(\Delta n/\lambda c E^2)_{E \rightarrow 0}$ . The specific Kerr constant is given in statvolt<sup>-2</sup> cm<sup>4</sup> g<sup>-1</sup> (1 statvolt<sup>-2</sup> cm<sup>4</sup> g<sup>-1</sup> = 1.113 × 10<sup>-10</sup> V<sup>-2</sup> m<sup>4</sup> kg<sup>-1</sup>).

Figure 2 illustrates the variation of

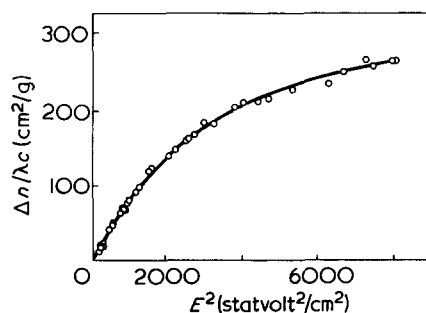


Figure 1 A plot of  $\Delta n/\lambda c$  versus  $E^2$  for sample II in 90 vol % ethylene glycol at 25°C ( $c = 1.8 \times 10^{-4}$  g/cm<sup>3</sup>).  $\circ$ , experimental values; —, theoretical curve calculated for  $n = 1$ ,  $2\pi(g_1 - g_2)/\bar{n}\rho\lambda = 400$  cm<sup>2</sup>/g and  $zeL/2kT = 0.102$  according to equations (1) and (2)

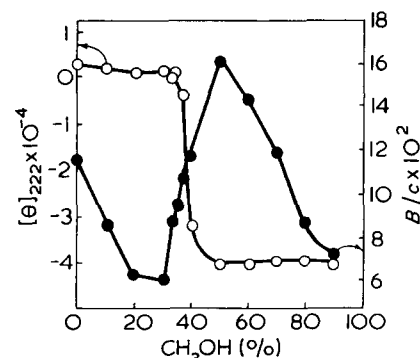


Figure 2 Specific Kerr constant (statvolt<sup>-2</sup> cm<sup>4</sup> g<sup>-1</sup>) and molar ellipticity at 222 nm (deg cm<sup>2</sup>/dmol) of sample I plotted against the volume percentage of methanol at 25°C ( $c = 1.8 \times 10^{-4}$  g/cm<sup>3</sup>, pH of aqueous solution = 6.8)

the specific Kerr constant ( $B/c$ ) and the molar ellipticity ( $[\theta]$ ) at 222 nm (one of the two negative extrema characteristic of  $\alpha$ -helix) with the solvent composition of water/methanol mixtures. With an increase in methanol content, the molar ellipticity undergoes a rather abrupt change which indicates a coil-to-helix transition. The specific Kerr constant decreases with increasing methanol content and rises suddenly in the region of helix-coil transition. After the helix is completed, the specific Kerr constant decreases again with increasing methanol content. The electric birefringence of the helical conformation in 90 vol % methanol is smaller than that of the coil form in water at low fields, but becomes larger in high fields. This means that the optical anisotropy factor of the helix is larger than that of the coil form as in the case of poly(L-lysine hydrobromide) in water/methanol mixtures<sup>10</sup>.

Figure 3 shows the specific Kerr constant and the molar ellipticity at 222 nm as functions of the solvent composition of water/ethylene glycol mixtures. In this case, the coil-to-helix transition takes place more gradually at higher contents of ethylene glycol. The helix-stabilizing effect of ethylene glycol appears to be weaker than that of methanol.

The high viscosity of ethylene glycol enables us to register accurately the rise and decay curves of the electric birefringence of sodium poly(L-glutamate) in 90 vol % ethylene glycol. Now, the ratio of the area above the rise curve and that below the decay curve gives a clue to the mechanism of electrical orientation<sup>8,11</sup>. In the limiting low fields this ratio is equal to unity for the induced dipole moment orientation and equal to four for the permanent dipole moment orientation. In the case of our system in 90 vol % ethylene glycol the area ratio increased with decreasing field strength and approached unity in the limit. Thus the transient behaviour indicates that the induced dipole moment (probably due to the counterion atmosphere polarization) dominates in the orienting mechanism.

The field strength dependence of the steady-state birefringence is also closely related to the orienting mechanism. The electric birefringence of a dilute solution of axially symmetric, rigid macromolecules is expressed by:

$$\Delta n/\lambda c = (2\pi/\bar{n}\rho\lambda)(g_1 - g_2)\Phi(E) \quad (1)$$

where  $\bar{n}$  is the average refractive index

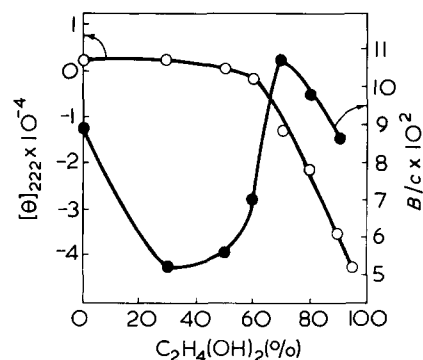


Figure 3 Specific Kerr constant and molar ellipticity at 222 nm of sample I plotted against the volume percentage of ethylene glycol at 25°C ( $c = 1.5 \times 10^{-4}$  g/cm<sup>3</sup>, pH of aqueous solution = 6.7)

of the solution,  $\rho$  is the density of the solute,  $g_1 - g_2$  is the optical anisotropy factor and  $\Phi$  is the orientation factor which describes the degree of orientation and is a function of the field strength<sup>12,13</sup>. Recently we have derived a theoretical equation for the orientation factor of rod-like polyelectrolytes on the basis of Mandel's model<sup>14</sup>. In this model<sup>15</sup> the polyion is assumed to be a thin rigid rod of length  $L$  with uniformly distributed charges. The number of counterions, per polyion, which are bound but mobile in the longitudinal direction is denoted by  $n$ . If the interactions between the counterions are neglected, the orientation factor is given by:

$$\Phi = \frac{\int_0^1 u^2 \left( \frac{\sinh \kappa u}{\kappa u} \right)^n du}{2 \int_0^1 \left( \frac{\sinh \kappa u}{\kappa u} \right)^n du} - \frac{1}{2} \quad (2)$$

with

$$u = \cos \theta \quad (3)$$

$$\kappa = zeLE/2kT \quad (4)$$

where  $z$  is the valence of the counterion,  $e$  is the elementary charge,  $k$  is the Boltzmann constant and  $T$  is the temperature. According to equation (2), the effect of saturation of the ion atmosphere polarization on the orientation factor becomes notable only when  $n$  is sufficiently small<sup>14</sup>.

Figure 1 shows a plot of  $\Delta n/\lambda c$  versus  $E^2$  for the helical conformation

of sodium poly(L-glutamate) in 90 vol % ethylene glycol. In order to fit this plot to equations (1) and (2), a value of  $n$  as small as unity has to be selected. The solid curve in this Figure is a theoretical curve with  $n = 1$  obtained by assigning appropriate values to the two parameters,  $2\pi(g_1 - g)/\bar{n}\rho\lambda$  and  $zeL/2kT$ . The agreement between theory and experiment is fairly good. However, such a small value of  $n$  is unrealistic. We must take into account the counterion-counterion repulsion to get rid of this difficulty.

#### Acknowledgements

This work was supported by research grants from the Ministry of Education of Japan, to which the authors wish to

express their gratitude.

Katsumi Takakusaki,  
Kazuo Kikuchi  
and Koshiro Yoshioka

Department of Chemistry,  
College of General Education,  
University of Tokyo, Meguroku,  
153 Tokyo, Japan  
(Received 9 May 1977)

#### References

- 1 Yamaoka, K. *PhD Thesis* University of California (1964)
- 2 Matsumoto, M., Watanabe, H. and Yoshioka, K. *Biopolymers* 1968, 6, 929; 1970, 9, 1307; 1973, 12, 1729
- 3 Doty, P., Wada, A., Yang, J. T. and Blout, E. R. *J. Polym. Sci.* 1957, 23, 851
- 4 Kobayasi, S. and Ikegami, A.

- 5 *Biopolymers* 1975, 14, 543
- 6 Iizuka, E. and Yang, J. T. *Biochemistry* 1965, 4, 1249
- 7 Tiffany, M. L. and Krimm, S. *Biopolymers* 1968, 6, 1379
- 8 Wada, A. *Mol. Phys.* 1960, 3, 409
- 9 Yoshioka, K. and Watanabe, H. 'Physical Principles and Techniques of Protein Chemistry, Part A', (Ed. S. Leach), Academic Press, New York, 1969, p 335
- 10 Kikuchi, K. and Yoshioka, K. *J. Phys. Chem.* 1973, 77, 2101
- 11 Kikuchi, K. and Yoshioka, K. *Biopolymers* 1973, 12, 2667
- 12 Yoshioka, K. and Watanabe, H. *Nippon Kagaku Zasshi* 1963, 84, 626
- 13 Peterlin, A. and Stuart, H. A. *Z. Phys.* 1939, 112, 129
- 14 O'Konski, C. T., Yoshioka, K. and Orttung, W. H. *J. Phys. Chem.* 1959, 63, 1558
- 15 Kikuchi, K. and Yoshioka, K. *Biopolymers* 1976, 15, 583
- 16 Mandel, M. *Mol. Phys.* 1961, 4, 489

### Characterization of urea-formaldehyde adducts and resins by $^{13}\text{C}$ -n.m.r. spectroscopy

#### Introduction

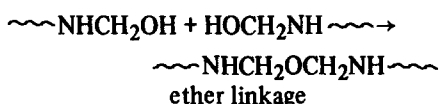
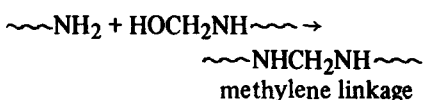
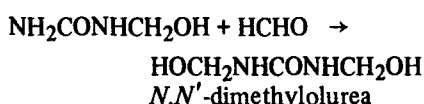
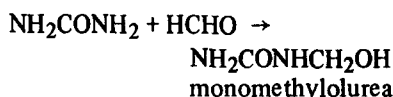
Despite the continuing development of new polymeric materials, well-established thermosetting resins such as urea-formaldehyde, melamine-formaldehyde and phenol-formaldehyde resins continue to enjoy widespread use as moulding compounds, surface coatings, adhesives and in laminates. Phenol-formaldehyde resins have been extensively studied, but urea-formaldehyde and melamine-formaldehyde systems have been less well characterized although the classical work of de Jong and de Jonge<sup>1</sup> has helped to elucidate the nature of the reactions that occur in the early stages of resin formation. Urea-formaldehyde adducts and resins have also been characterized by infrared spectroscopy<sup>2,3</sup>, chromatographic techniques<sup>4-6</sup> and more recently, by proton magnetic resonance<sup>7-9</sup>.

This paper describes some preliminary results of a study of some urea-formaldehyde adducts and resins using  $^{13}\text{C}$ -n.m.r. spectroscopy and represents, as far as we are aware, the first reported application of this technique to the urea-formaldehyde system.

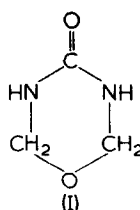
#### Chemistry of urea-formaldehyde resin formation

The chemistry of urea-formaldehyde resin formation has been discussed in some detail by Vale and Taylor<sup>10</sup>. The formation of low molecular weight resins is believed to occur via the prior

formation of methylolureas followed by condensation of these to give short linear and branched chains containing ether and methylene linkages. The more important reactions are indicated below:



Other products which have been identified in urea-formaldehyde systems include  $N,N$ -dimethylolurea [ $\text{NH}_2\text{CON}(\text{CH}_2\text{OH})_2$ ], trimethylolurea [ $\text{HOCH}_2\text{NHCON}(\text{CH}_2\text{OH})_2$ ] and uron (I) and its derivatives:



#### Experimental

**Materials.** Aqueous formaldehyde solutions (formalin) were freshly prepared (and thus contained no methanol) by heating paraformaldehyde in a stream of nitrogen and passing this gas stream into distilled water (or  $\text{D}_2\text{O}$ ) at  $\sim 25^\circ\text{C}$ . The formaldehyde contents of the resulting solutions (normally 30% w/w) were determined by iodometry<sup>11</sup>. 'Analar' grade urea was used without further purification.

#### Preparation of model compounds.

The following model compounds were prepared as apparently pure crystalline compounds by literature methods: monomethylolurea<sup>12</sup>,  $N,N'$ -dimethylolurea<sup>12</sup>, methylene diurea<sup>12</sup>, dimethyloloxymethylene diurea (II)<sup>13</sup>, the monomethylether of monomethylolurea<sup>14</sup>, the dimethylether of dimethylolurea<sup>14</sup>, tetraethylidimethylene diureid (III)<sup>14</sup>, uron<sup>15</sup> and the dimethylether of dimethyloluron (IV)<sup>14</sup>:

